

Contributions to the Muon's Anomalous Magnetic Moment from a Hidden Sector

David McKeen*

*Enrico Fermi Institute and Department of Physics,
University of Chicago, 5640 South Ellis Avenue, Chicago, IL 60637*

(Dated: July 13, 2021)

The measurement of the anomalous magnetic moment of the muon provides a stringent test of the standard model and of any physics that lies beyond it. There is currently a deviation of 3.1σ between the standard model prediction for the muon's anomalous magnetic moment and its experimental value. We calculate the contribution to the anomalous magnetic moment in theories where the muon couples to a particle in a hidden sector (that is, uncharged under the standard model) and a connector (which has nontrivial standard model gauge and hidden sector quantum numbers).

PACS numbers: 12.60.-i, 13.40.Em, 14.60.Hi, 14.80.-j

I. INTRODUCTION

Quantum field theory predicts that the gyromagnetic ratio of the muon will differ slightly from its tree-level value of $g_\mu = 2$. Properly accounting for the nonzero value of the anomalous magnetic moment, $a_\mu = (g_\mu - 2)/2$, of the muon is a precise test of the standard model (SM) and of physics beyond the SM.

The most recent determination of a_μ in the SM is [1]

$$a_\mu^{\text{SM}} = (11\,659\,183.4 \pm 4.9) \times 10^{-10} \quad . \quad (1)$$

The dominant sources of uncertainty in this expression are the leading-order hadronic vacuum polarization contribution and the contribution from hadronic light-by-light scattering. In Ref. [1], the leading-order hadronic contribution is determined to be

$$a_\mu^{\text{LO Had.}} = (695.5 \pm 4.1) \times 10^{-10} \quad , \quad (2)$$

while the most recent determination of the hadronic light-by-light contribution is [2]

$$a_\mu^{\text{Had. LbL}} = (10.5 \pm 2.6) \times 10^{-10} \quad . \quad (3)$$

The total SM prediction for a_μ in Eq. 1 differs from the experimental value [3],

$$a_\mu^{\text{Exp}} = (11\,659\,208.0 \pm 5.4 \pm 3.3) \times 10^{-10} \quad , \quad (4)$$

at the 3.1σ level. There is some discrepancy in using e^+e^- or τ decay data to extract the leading-order hadronic contribution to a_μ with τ decay data leading to a 1.9σ difference between the SM and experimental values of a_μ . For recent reviews of the status of a_μ , see Ref. [4]

The difference between a_μ^{SM} and a_μ^{Exp} has spurred numerous studies of new physics scenarios that could offer an explanation, for example, supersymmetry [5], universal extra dimensions [6], and unparticles [7]. Another scenario that has received attention in the literature is that of a hidden $U(1)'$ whose gauge boson kinetically mixes with the photon [8]. The constraints from a_μ on such a scenario are discussed in [9].

In this paper we investigate and catalogue the contributions to a_μ that arise from the muon coupling to some hidden sector. We do this in four situations that differ in the spin of the hidden sector particle that couples to the muon, and in the spin of other particles present in the interaction to preserve gauge invariance. These scenarios are generalizations of some models already investigated, like that of [9].

Schematically, the interactions we consider are of the form

$$\mathcal{L}_{\text{int}} \sim \lambda XY\mu \quad , \quad (5)$$

*Electronic address: mckeen@theory.uchicago.edu

where Lorentz and gauge indices have been suppressed. In this Lagrangian and in the rest of this work, X refers to a SM singlet that could be charged under some hidden symmetry group, which we denote by G , and Y is a particle that is charged under the SM (to preserve the SM gauge invariance of the interaction) and under G if X is (to preserve G invariance). The particles in Eq. 5 are classified in the table below:

Type of matter	Std. Model	G	Example
Ordinary	Non-singlet	Singlet	μ
Connector	Non-singlet	Non-singlet	Y
Hidden	Singlet	Non-singlet	X

λ is the coupling strength of this interaction between the muon, the hidden sector particle X , and the connector Y . Interactions of this form generate corrections to a_μ of order λ^2 .

We note that X could be a dark matter candidate. If $m_X < m_Y$ and X is the lightest particle with some hidden charge, it could be long lived. Indeed, the relic density of X could naturally be driven to the observed value of $\Omega_X \simeq 0.23$ although its mass is unconnected to the electroweak scale in a WIMPless dark matter scenario [10]. For X to be a viable dark matter candidate, it cannot be coupled too strongly to the SM; that is $\lambda \lesssim g_{\text{weak}}$. Of course, this condition is relaxed if we do not require that X comprise the most of the dark matter density. These scenarios have been studied in situations where X couples to b quarks, leading to an explanation of the DAMA/LIBRA signal [11] and to missing energy in decays of mesons with b quarks [12].

In Sec. II, we discuss constraints on X and Y from collider experiments. In Sec. III, we present the contributions to a_μ due to several scenarios of the form of Eq. 5. We discuss constraints from the measured value of a_μ on these scenarios in Sec. IV, and, in Sec. V, we conclude.

II. COLLIDER CONSTRAINTS ON X AND Y

If X is a SM singlet that is only weakly coupled to the SM, as we assume here, then there are no firm constraints on its allowed mass coming from collider experiments. We consider its mass to be essentially free in this study.

There are, however, tight bounds on the possible mass of Y since it has the same electric charge as the muon. The firmest bounds come from the LEP experiments' searches for right-handed sleptons. These experiments looked for a pair of sleptons produced by a virtual photon or Z that decay to a pair of acoplanar leptons along with two neutralinos (missing energy). Such searches apply in the case of a Lagrangian of the form of Eq. 5 if $m_X < m_Y - m_\mu$ and λ large enough that the Y 's decay promptly, that is, $\lambda \gtrsim 10^{-8}$.

The ALEPH, DELPHI, L3, and OPAL experiments set a combined limit [13] on the production of smuons decaying to muons and missing energy of

$$\sigma(e^+e^- \rightarrow \tilde{\mu}_R \bar{\tilde{\mu}}_R) < 0.08 \text{ pb} \quad \text{at 95\% C.L.} \quad (6)$$

if $\mathcal{B}(\tilde{\mu}_R \rightarrow \chi_1^0 \mu^-) = 1$ for $m_{\tilde{\mu}_R} \lesssim 95$ GeV and $m_{\tilde{\mu}_R} - m_{\chi_1^0} \gtrsim 10$ GeV at a rescaled center-of-mass energy $\sqrt{s} = 208$ GeV. If $m_X \lesssim m_Y + 10$ GeV and $Y \rightarrow X\mu$ is the dominant decay mode for Y , then this limit should also hold for Y pair production, assuming acceptances don't differ too drastically.

In this paper we will consider a fermionic Y in Secs. III A and III B, a scalar Y in Sec. III C, and a vector Y in III D. In any of these cases, Y has the same electric charge as the muon since X is assumed to be electrically neutral. Its charges under electroweak $SU(2)_L \times U(1)_Y$ depend on whether the interaction of Eq. 5 respects electroweak symmetry. Of course, what electroweak charges we assign to Y are important in estimating the production cross section at LEP.

In the case of a fermionic Y , the simplest case is that of a heavy chiral lepton whose $SU(2)_L \times U(1)_Y$ charges are the same as that of the muon. The production cross section, $\sigma(e^+e^- \rightarrow \gamma^* Z^* \rightarrow Y\bar{Y})$, is calculated in Sec. A 1 and is plotted in Fig. 1 (a).

A scalar Y could either couple to μ_L or μ_R . We label each of these as Y_L and Y_R respectively, where the subscript does not indicate any chirality for Y since it has none, but the chirality of the muon to which it couples. This is the situation with sleptons where, for example, $\tilde{\mu}_L$ and $\tilde{\mu}_R$ are different states. Y_L and Y_R each have unit electric charge which fixes their couplings to photons. We also choose that Y_L couples in a gauge invariant way to Z bosons with the same strength as μ_L and similarly for Y_R . The production cross sections, $\sigma(e^+e^- \rightarrow \gamma^* Z^* \rightarrow Y_L^+ Y_L^-)$ and $\sigma(e^+e^- \rightarrow \gamma^* Z^* \rightarrow Y_R^+ Y_R^-)$, are derived in Sec. A 2 and are plotted in Fig. 1 (b).

The situation where Y is a vector boson is more complicated as further states need to be introduced to maintain unitarity. As in the scalar case, there are again two Y s which we label in terms of the handedness of the muon that they couple to, Y_L^ν and Y_R^ν . These vector bosons are electrically charged which again fixes their coupling to photons. If this is the only coupling that contributes to Y pair production, then the cross section $\sigma(e^+e^- \rightarrow \gamma^* \rightarrow Y_{L,R}^{\nu+} Y_{L,R}^{\nu-})$

diverges as the center-of-mass energy increases, in conflict with unitarity. Only adding in a coupling of $Y_{L,R}^\nu$ to the Z does not fix this since the Z has a chiral coupling to leptons while the photon's is vector-like. This is the same problem faced when calculating $\sigma(e^+e^- \rightarrow W^{\nu+}W^{\nu-})$. The solution there is to include t -channel neutrino exchange in addition to s -channel photon and Z exchange. We consider the case where the solution to the unitarity problem in vector Y pair production is similar; we assume that there are fermions, N_L and N_R , which are electrically neutral that are exchanged in the t -channel. This is the case if, for example, Y_R^ν is a heavy charged gauge boson associated with a broken $SU(2)_R$ and N_R is a right-handed neutrino. A similar situation occurs in little Higgs models with T-Parity where we can consider Y_L^ν as a T-odd vector boson and N_L as a T-odd neutrino. N_L or N_R could also be thought of as the singlet in an interaction of the form of that in Eq. 5 with the muon replaced by the electron. In any one of these scenarios, the requirement that the production cross section eventually vanishes as the center-of-mass energy grows implies some relationships between the couplings of $Y_{L,R}^\nu$ to the Z and to $e_{L,R} - N_{L,R}$. The cross sections $\sigma(e^+e^- \rightarrow Y_L^{\nu+}Y_L^{\nu-})$ and $\sigma(e^+e^- \rightarrow Y_R^{\nu+}Y_R^{\nu-})$ are calculated in Sec. A3 and are shown for different masses of N_L and N_R in Figs. 1 (c) and (d). Since we do not assume anything about the coupling of $Y_{L,R}^\nu$ to quarks, the stringent limits on heavy charged vector bosons from hadron colliders are ignored.

In Fig. 1, it is seen that the Y^+Y^- production cross section is greater than 0.08 pb for $m_Y \gtrsim 89$ GeV in each of these cases. If Y is long-lived on detector time scales (m_X could be larger than m_Y or $\lambda \lesssim 10^{-8}$) then tracks would have been seen in the electromagnetic calorimeters in the LEP experiments as long as the center-of-mass energy was above Y threshold. We consider this scenario to be ruled out.

The situation is complicated if there are neutrinos with masses above $m_Z/2$ that are part of an $SU(2)_L$ doublet with Y_L or if lepton family violating decays compete with $Y \rightarrow X\mu$. However, searches for acoplanar e^+e^- or $\tau^+\tau^-$ pairs and missing energy yield similar limits on the production cross section of selectrons and staus. Therefore, in this work, we take a lower bound of $m_Y \gtrsim 89$ GeV.

If Y only receives SM contributions to its mass perturbativity could become an issue if $m_Y \gtrsim 500$ GeV. We do not explore this issue in detail.

III. CONTRIBUTIONS TO a_μ DUE TO INTERACTION OF THE MUON WITH A HIDDEN SECTOR

In this paper we investigate the consequences of the muon coupling to a standard model singlet, which we denote by X , and to a particle charged under the standard model, which we call Y . There are four cases we consider based on the intrinsic angular momenta of X and Y . The first case is a spin-0 X and a spin-1/2 Y . The second is a spin-1 X and a spin-1/2 Y . The third case is a spin-1/2 X and a spin-0 Y while the last is a spin-1/2 X and a spin-1 Y . We present the contributions to a_μ in each case below.

A. Case I

In the first case, the interaction Lagrangian is given by

$$\mathcal{L}_{\text{int}} = \lambda_L X \bar{Y}_R \mu_L + \lambda_R X \bar{Y}_L \mu_R + \text{H.c.} \quad (7)$$

This contributes to the muon's anomalous magnetic moment through the diagram seen in Fig. 2 (a). This contribution is easily calculated to be

$$(\Delta a_\mu)_1 = \frac{1}{16\pi^2} \int_0^1 dx \frac{(1-x)^2 [(\lambda_L^2 + \lambda_R^2) m_\mu m_Y + 2\lambda_L \lambda_R x m_\mu^2]}{(1-x)m_Y^2 + x m_X^2 - x(1-x)m_\mu^2} \quad (8)$$

If $m_Y, m_X \gg m_\mu$ then we can approximate this expression as

$$(\Delta a_\mu)_1 \simeq \frac{1}{16\pi^2} (\lambda_L^2 + \lambda_R^2) \int_0^1 dx \frac{(1-x)^2 m_\mu m_Y}{(1-x)m_Y^2 + x m_X^2} \quad (9)$$

$$= \frac{1}{32\pi^2} (\lambda_L^2 + \lambda_R^2) \frac{m_\mu}{m_Y} H_1 \left(\frac{m_X^2}{m_Y^2} \right) \quad (10)$$

$$= 8.36 \times 10^{-7} (\lambda_L^2 + \lambda_R^2) \left(\frac{400 \text{ GeV}}{m_Y} \right) H_1 \left(\frac{m_X^2}{m_Y^2} \right) \quad (11)$$

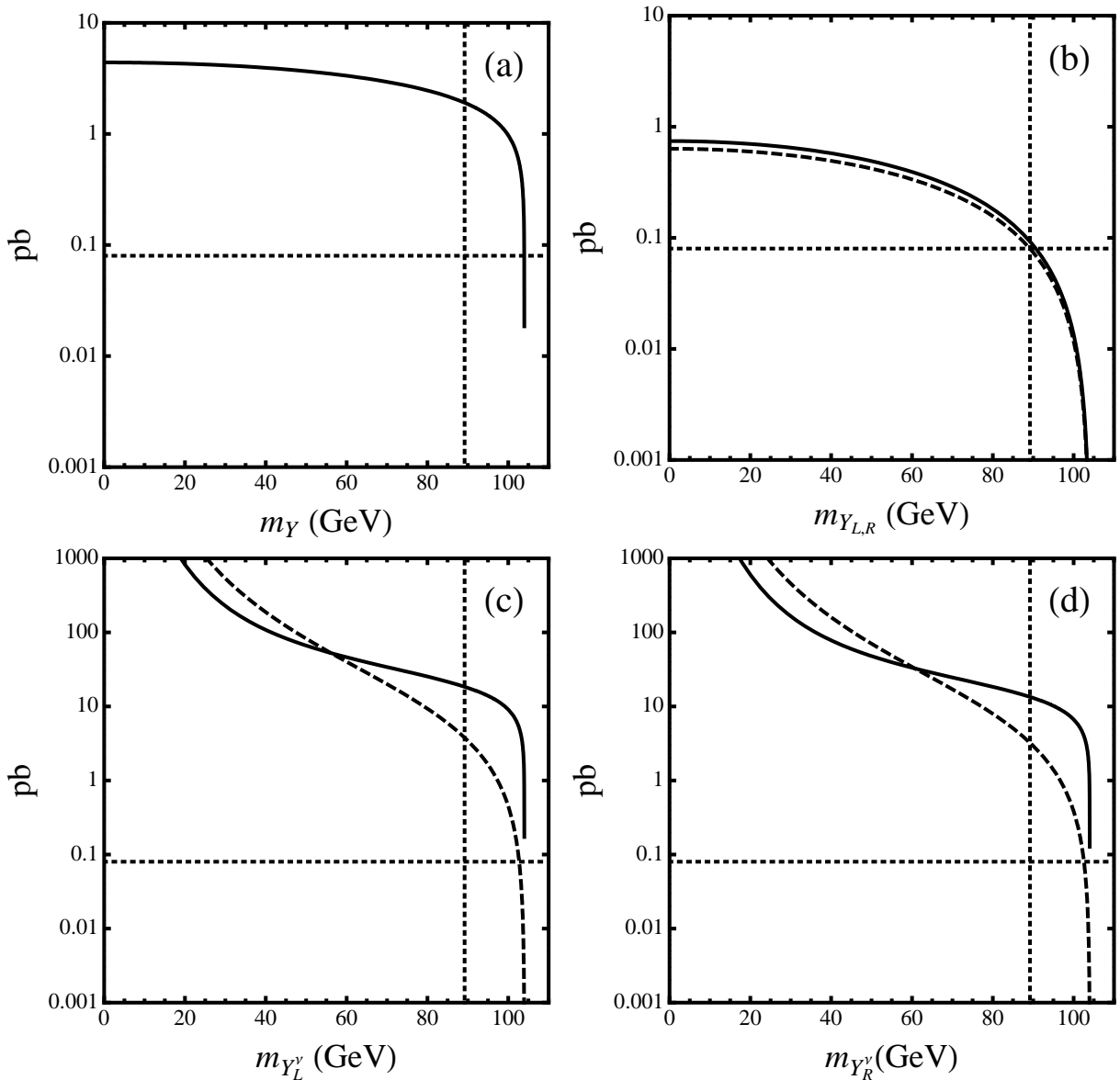


FIG. 1: (a) $\sigma(e^+e^- \rightarrow Y\bar{Y})$ at $\sqrt{s} = 208$ GeV where Y is a fermion. (b) $\sigma(e^+e^- \rightarrow Y_L^+Y_L^-)$ (solid) and $\sigma(e^+e^- \rightarrow Y_R^+Y_R^-)$ (dashed) at $\sqrt{s} = 208$ GeV where Y is a scalar. (c) $\sigma(e^+e^- \rightarrow Y_L^{\nu+}Y_L^{\nu-})$ where Y is a vector boson for $m_{N_L} = 0$ (solid) and $m_{N_L} = 10$ TeV (dashed). (d) $\sigma(e^+e^- \rightarrow Y_R^{\nu+}Y_R^{\nu-})$ where Y is a vector boson for $m_{N_R} = 0$ (solid) and $m_{N_R} = 10$ TeV (dashed). The horizontal dotted lines in each plot indicate the LEP limit of 0.08 pb and the vertical dotted lines indicate the lower bound on m_Y of 89 GeV which comes from scalar Y_R pair production as seen in (b). Note the p -wave suppression of the production of a scalar Y pair in (b) near threshold which causes its cross section to decrease more steadily as a function of increasing m_Y than the cusplike cross section for fermionic Y pair production in (a). We also see that for $m_{N_{L,R}} = 0$ in (c) and (d), there is no p -wave suppression of the cross section of a vector Y pair near threshold whereas when we decouple $N_{L,R}$ by taking its mass to 10 TeV, there is a p -wave suppression. This suppression can be seen in the expression for the production cross section in Sec. A 3; for $m_{N_{L,R}} \gg \sqrt{s}$, the cross section is proportional to β^3 .

where

$$H_1(r) = 2 \int_0^1 dx \frac{(1-x)^2}{1-(1-r)x} \quad . \quad (12)$$

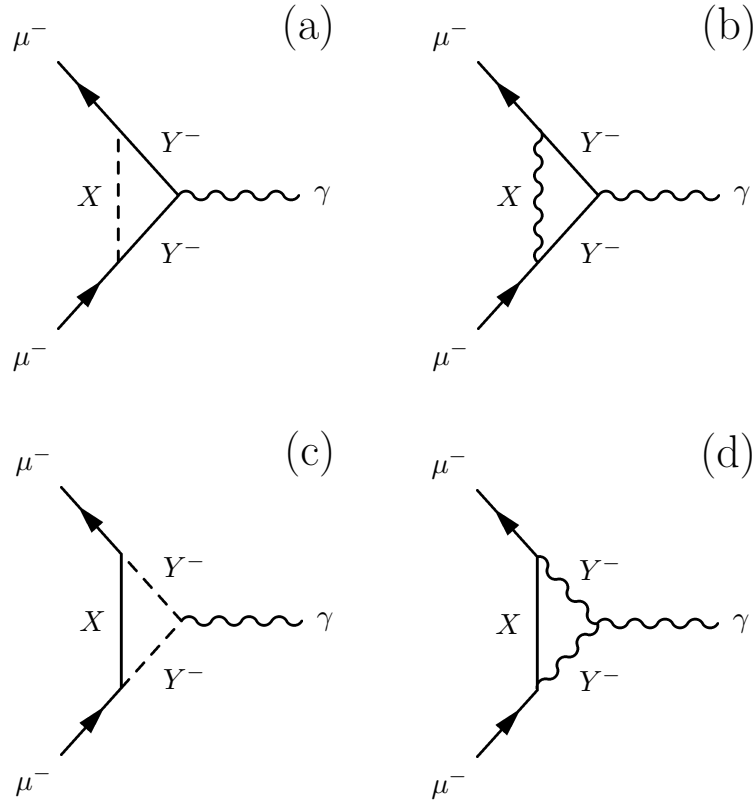


FIG. 2: Diagrams relevant for Cases I (a), II (b), III (c), IV (d).

B. Case II

In the second case, the interaction Lagrangian is now given by

$$\mathcal{L}_{\text{int}} = \lambda_L X^\mu \bar{Y}_L \gamma_\mu \mu_L + \lambda_R X^\mu \bar{Y}_R \gamma_\mu \mu_R + \text{H.c.} \quad . \quad (13)$$

This gives a contribution to a_μ through the diagram seen in Fig. 2 (b). We find

$$(\Delta a_\mu)_2 = \frac{1}{8\pi^2} \int_0^1 dx \frac{x(1-x) [4\lambda_L \lambda_R m_\mu m_Y - (\lambda_L^2 + \lambda_R^2) (1+x) m_\mu^2]}{(1-x)m_Y^2 + xm_X^2 - x(1-x)m_\mu^2} \quad (14)$$

$$+ \frac{1}{16\pi^2} \frac{m_\mu^2}{m_X^2} \int_0^1 dx \frac{(1-x)^3 [2\lambda_L \lambda_R (1-x) m_\mu m_Y - (\lambda_L^2 + \lambda_R^2) (m_Y^2 - xm_\mu^2)]}{(1-x)m_Y^2 + xm_X^2 - x(1-x)m_\mu^2} \quad (15)$$

If $m_Y, m_X \gg m_\mu$,

$$(\Delta a_\mu)_2 \simeq \frac{m_\mu m_Y}{2\pi^2} \lambda_L \lambda_R \int_0^1 dx \frac{x(1-x)}{(1-x)m_Y^2 + xm_X^2} - \frac{m_\mu^2 m_Y^2}{16\pi^2 m_X^2} (\lambda_L^2 + \lambda_R^2) \int_0^1 dx \frac{(1-x)^3}{(1-x)m_Y^2 + xm_X^2} \quad (16)$$

$$= \frac{1}{4\pi^2} \lambda_L \lambda_R \left(\frac{m_\mu}{m_Y} \right) H_2 \left(\frac{m_X^2}{m_Y^2} \right) \quad (17)$$

$$- \frac{1}{48\pi^2} (\lambda_L^2 + \lambda_R^2) \frac{m_\mu^2}{m_X^2} G_2 \left(\frac{m_X^2}{m_Y^2} \right) \quad (18)$$

$$= 6.69 \times 10^{-6} \lambda_L \lambda_R \left(\frac{400 \text{ GeV}}{m_Y} \right) H_2 \left(\frac{m_X^2}{m_Y^2} \right) \quad (19)$$

$$- 2.36 \times 10^{-5} (\lambda_L^2 + \lambda_R^2) \left(\frac{1 \text{ GeV}}{m_X} \right)^2 H_2 \left(\frac{m_X^2}{m_Y^2} \right) , \quad (20)$$

where

$$H_2(r) = 2 \int_0^1 dx \frac{x(1-x)}{1-(1-r)x} , \quad (21)$$

$$G_2(r) = 3 \int_0^1 dx \frac{(1-x)^3}{1-(1-r)x} , \quad (22)$$

This interaction is a generalization of the much-discussed case in which the photon kinetically mixes with a GeV scale gauge boson. To obtain the contribution to the muon's anomalous magnetic moment in this situation, we identify Y with the muon and write $\lambda_L = \lambda_R = \epsilon e$ where ϵ characterizes the strength of the kinetic mixing and e is the strength of the muon's electric charge. Then (as in [9]),

$$(\Delta a_\mu)_{2'} = \frac{\epsilon^2 \alpha m_\mu^2}{\pi} \int_0^1 dx \frac{x(1-x)^2}{(1-x)^2 m_\mu^2 + xm_X^2} \quad (23)$$

If $m_X \gg m_\mu$ we can approximate this as

$$(\Delta a_\mu)_{2'} \simeq \frac{\epsilon^2 \alpha}{3\pi} \left(\frac{m_\mu}{m_X} \right)^2 \quad (24)$$

$$= 8.65 \times 10^{-6} \epsilon^2 \left(\frac{1 \text{ GeV}}{m_X} \right)^2 , \quad (25)$$

while if $m_X \ll m_\mu$,

$$(\Delta a_\mu)_{2'} \simeq \frac{\epsilon^2 \alpha}{2\pi} \quad (26)$$

$$= 1.16 \times 10^{-3} \epsilon^2 . \quad (27)$$

These expressions agree with those in Ref. [9].

C. Case III

X is now a fermion, while Y is a scalar. The interaction is given by

$$\mathcal{L}_{\text{int}} = \lambda_L Y_L \bar{X} \mu_L + \lambda_R Y_R \bar{X} \mu_R + \text{H.c.} . \quad (28)$$

Here, the subscript on Y labels the helicity of the muon to which it couples and nothing about its own helicity, just as the subscripts that label sfermions in supersymmetry do. In Cases I and II, Y_L and Y_R were two-component Weyl

spinors married to form a Dirac fermion whose mass term breaks electroweak symmetry. Here, they are separate fields that, in general, have different masses. The diagram shown in Fig. 2 (c) gives a contribution to a_μ of

$$(\Delta a_\mu)_3 = \frac{\lambda_L^2}{16\pi^2} \int_0^1 dx \frac{x(1-x)m_\mu m_X}{(1-x)m_{Y_L}^2 + xm_X^2 - x(1-x)m_\mu^2} + (L \rightarrow R) \quad . \quad (29)$$

If $m_Y, m_X \gg m_\mu$ then we can approximate this expression as

$$(\Delta a_\mu)_3 \simeq \frac{m_\mu m_X}{32\pi^2} \left[\frac{\lambda_L^2}{m_{Y_L}^2} H_2 \left(\frac{m_X^2}{m_{Y_L}^2} \right) + \frac{\lambda_R^2}{m_{Y_R}^2} H_2 \left(\frac{m_X^2}{m_{Y_R}^2} \right) \right] \quad (30)$$

$$= 2.09 \times 10^{-9} \left[\lambda_L^2 \left(\frac{400 \text{ GeV}}{m_{Y_L}} \right)^2 H_2 \left(\frac{m_X^2}{m_{Y_L}^2} \right) + \lambda_R^2 \left(\frac{400 \text{ GeV}}{m_{Y_R}} \right)^2 H_2 \left(\frac{m_X^2}{m_{Y_R}^2} \right) \right] \left(\frac{m_X}{1 \text{ GeV}} \right) \quad , \quad (31)$$

where H_2 is defined in Eq. 22.

D. Case IV

The last case we consider is a fermionic X and a spin-1 Y . The interaction is now

$$\mathcal{L}_{\text{int}} = \lambda_L Y_L^\nu \bar{X} \gamma_\nu \mu_L + \lambda_R Y_R^\nu \bar{X} \gamma_\nu \mu_R + \text{H.c.} \quad . \quad (32)$$

As in Case III, the subscript on Y only labels the muon to which it couples. The relevant diagram is shown in Fig. 2 (d). In this case the contribution to a_μ is

$$(\Delta a_\mu)_4 = \frac{\lambda_L^2}{8\pi^2} \int_0^1 dx \frac{(1-x)^2(2-x)m_\mu^2}{(1-x)m_{Y_L}^2 + xm_X^2 - x(1-x)m_\mu^2} + \mathcal{O} \left(\frac{m_\mu^2}{m_{Y_L}^2} \right) + (L \rightarrow R) \quad . \quad (33)$$

If $m_Y, m_X \gg m_\mu$ then we can approximate this expression as

$$(\Delta a_\mu)_4 \simeq \frac{\lambda_L^2}{8\pi^2} \frac{m_\mu^2}{m_{Y_L}^2} \int_0^1 dx \frac{(1-x)^2(2-x)}{1-x+x(m_X^2/m_{Y_L}^2)} + (L \rightarrow R) \quad (34)$$

$$= 7.36 \times 10^{-10} \left[\lambda_L^2 \left(\frac{400 \text{ GeV}}{m_{Y_L}} \right)^2 H_4 \left(\frac{m_X^2}{m_{Y_L}^2} \right) + \lambda_R^2 \left(\frac{400 \text{ GeV}}{m_{Y_R}} \right)^2 H_4 \left(\frac{m_X^2}{m_{Y_R}^2} \right) \right] \quad , \quad (35)$$

where

$$H_4(r) = \frac{6}{5} \int_0^1 dx \frac{(1-x)^2(2-x)}{1-(1-r)x} \quad . \quad (36)$$

IV. COMPARISON WITH EXPERIMENT

The deviation of the standard model and experimental values for a_μ is

$$\Delta a_\mu = a_\mu^{\text{Exp}} - a_\mu^{\text{SM}} = (24.6 \pm 8.0) \times 10^{-10} \quad . \quad (37)$$

This discrepancy could be lessened if additional sources contribute to the muon's anomalous magnetic moment, as in the cases above. In Fig. 3 we plot the contribution to a_μ in each of the four cases as functions of m_X while fixing $\lambda_L = 0.1$, $\lambda_R = 0$, and $m_Y = 400 \text{ GeV}$ in Cases I and II, and $m_{Y_L} = 400 \text{ GeV}$ in Cases III and IV. In Case II, we have actually plotted $-(\Delta a_\mu)_2$, since, for these parameter choices, it is negative. We see that the helicity flip along the fermion line gives a factor of m_X in Case III, which suppresses its contributions to a_μ at small m_X for fixed m_{Y_L} . For smaller values of m_X , Case II gives a larger contribution to a_μ than in any of the other scenarios. We note that the contributions to a_μ for a fermionic X are generally smaller than for a bosonic X , given the same value of the coupling.

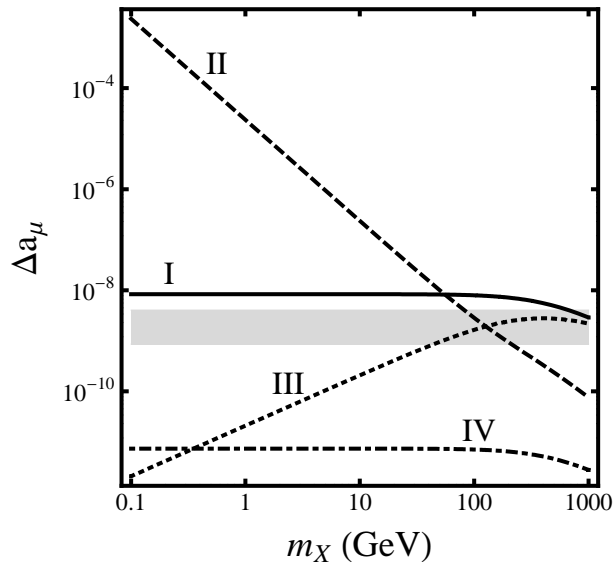


FIG. 3: Contributions to a_μ as functions of m_X for $\lambda_L = 0.1$, $\lambda_R = 0$, and $m_Y = 400$ GeV in Cases I (solid), II (dashed), III (dotted) and IV (dot-dashed). Note that we have plotted $-(\Delta a_\mu)_2$ in Case II (dashed) since it is negative for these choices of $\lambda_{L,R}$. We use the full one loop expressions for $(\Delta a_\mu)_1, \dots, (\Delta a_\mu)_4$. The light gray band shows values of Δa_μ for which the discrepancy between the theoretical and experimental values of a_μ (Eq. 37) is reduced to 1σ .

If any one of these scenarios describes the dominant contribution to the muon's anomalous magnetic moment beyond the standard model, we can ask what values of $\lambda_{L,R}$ for a given m_X and m_Y reduce the difference between the experimental and theoretical values of a_μ to less than 2σ . Fixing $\lambda_R = 0$ and $m_Y = 400$ GeV in Cases I and II, and $m_{Y_L} = 400$ GeV in Cases III and IV, we plot such values of λ_L as functions of m_X in Fig. 4. As we expect from Fig. 3, λ is constrained to smaller values in Cases I and II than in III and IV. Also, we note that in Case III, the contribution to a_μ is proportional to m_X , which suppresses it for low values of m_X .

We also show the contribution to a_μ as functions of m_X with $\lambda = \epsilon e = 0.06$ in Case II with Y identified as the muon in Fig. 5. Also shown are allowed values of ϵ as function of m_X .

We note that a fermionic X (Cases III and IV) can be more strongly coupled to muons without violating experimental constraints on a_μ if its mass is much smaller than that of Y . If Y 's are observed at the Tevatron or at the LHC, their decay widths can be compared with their contribution to a_μ to help determine their spin.

V. CONCLUSIONS

The experimental value of a_μ and its value in the SM currently differ at the 3.1σ level. This could be a sign of physics beyond the SM. Hidden sectors that couple to muons can provide an explanation of this deviation. In particular, situations in which the muon is coupled to particles that are charged under both the SM and a hidden symmetry group, G , and to particles only charged under G could give rise to a nonzero Δa_μ . These particles could also be found in collider experiments and measurements of their spins and couplings could shed light on the possibility that they contribute significantly to a_μ .

The spins of the hidden or mixed particles that couple to the muon greatly affect the structure of their contributions to a_μ . In particular, when a fermionic SM singlet is coupled to the muon with a bosonic connector, the constraints on the coupling strength from a_μ are less severe for SM singlet masses less than about 100 GeV. In this way, it is easier to “hide” a light fermionic SM singlet that couples to the muon than a bosonic one.

It is also worth considering whether couplings of the form of Eq. 5, in the case where X is a dark matter candidate, could be responsible for the recent excesses seen in cosmic ray positrons seen by the PAMELA experiment [14]. Depending on the values of λ_L and λ_R , the dominant annihilation channel for X 's could be $XX \rightarrow \mu^+\mu^-$ through t -channel Y exchange. Dark matter decays into a pair of muons are seen to fit the positron data reasonably well (modulo boost factors) [15], while the muons are kinematically constrained from producing baryons and so would not violate experimental limits on the antiproton fraction of cosmic rays. Future work will study this in more detail.

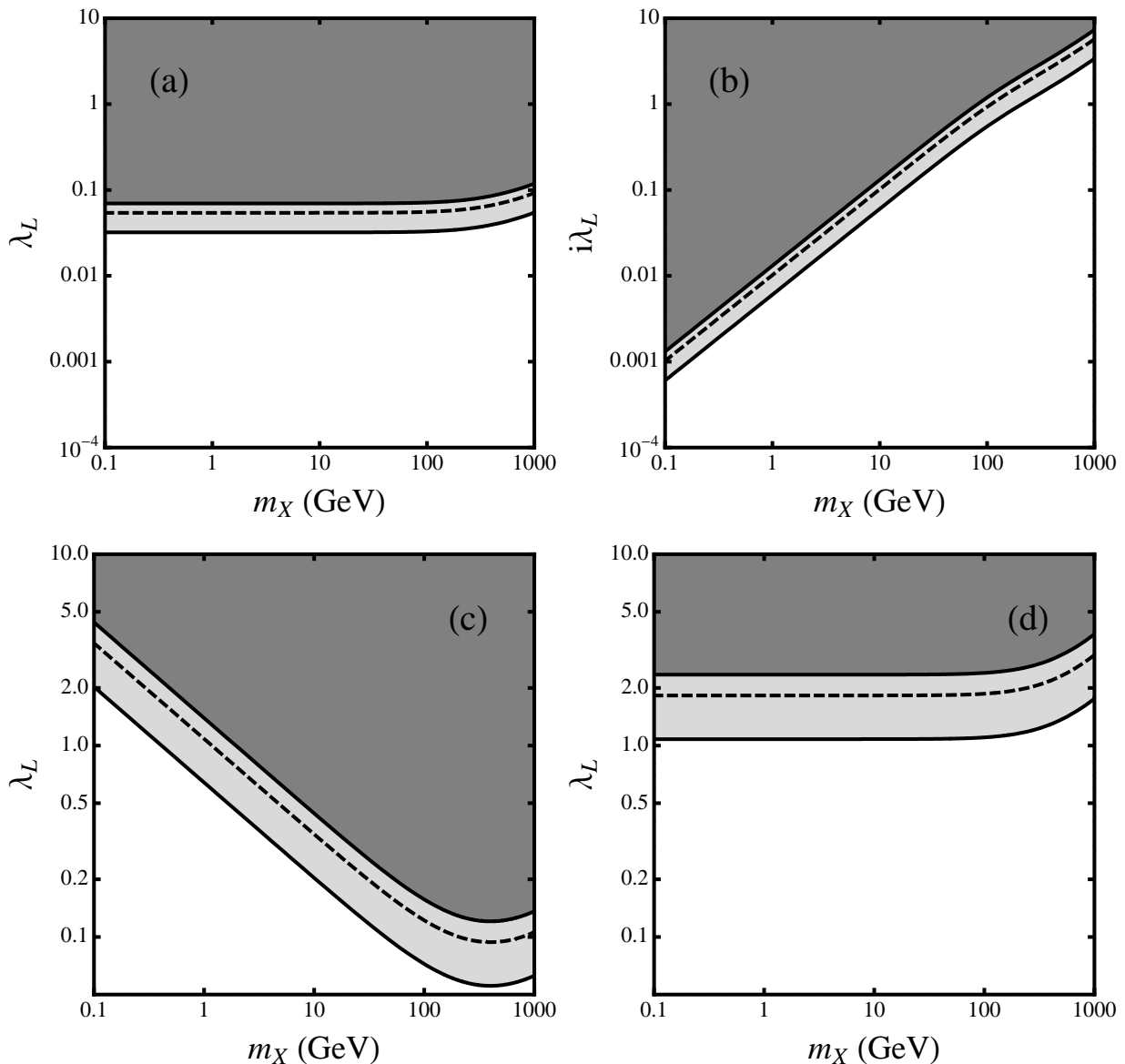


FIG. 4: Allowed values of λ_L in the situation where X and Y couple only to μ_L , $\lambda_R = 0$, as a function of m_X for $m_Y = 400$ GeV in Cases I (a) and II (b) and $m_{Y_L} = 400$ GeV in Cases III (c) and IV (d). In Case II (b), we plot $i\lambda_L$ since a real λ_L would give a negative $(\Delta a_\mu)_2$. We use the full one loop expressions for $(\Delta a_\mu)_1, \dots, (\Delta a_\mu)_4$. The light gray bands indicate values of λ and m_X for which the discrepancy between the theoretical and experimental values of a_μ is reduced to less than 2σ . The dashed lines show the values of λ and m_X where this discrepancy is 0σ . The dark gray regions contain points where the theoretical value of a_μ is at least 2σ larger than the experimental value. The unshaded regions show points where the experimental value of a_μ remains at least 2σ larger than the theoretical value.

A proposed muon ($g - 2$) experiment hopes to reduce the current experimental error on a_μ by a factor ~ 4 [16]. The uncertainty on the difference between the theoretical and experimental values would then be dominated by the theoretical errors. Such a measurement would help to determine the significance of the deviation between experimental and theoretical values of the muon's anomalous magnetic moment which is a powerful probe of physics beyond the SM.

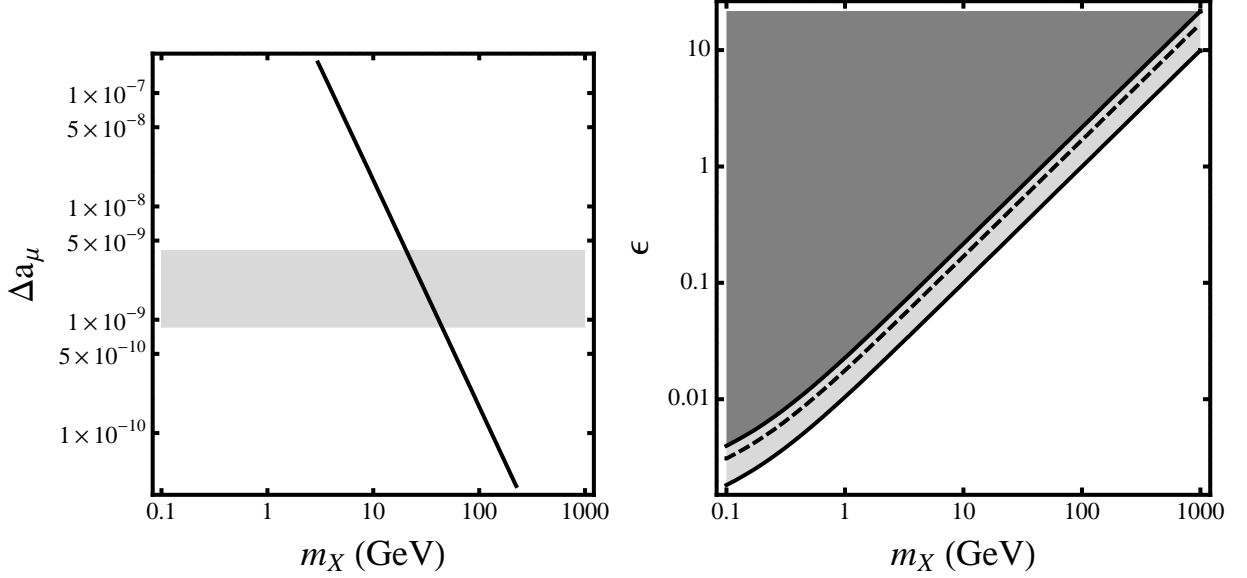


FIG. 5: Left: Contribution to a_μ as functions of m_X for $\lambda = \epsilon e = 0.06$ or $\epsilon \simeq 0.2$ in Case II with Y identified as the muon. The light gray band shows values of a_μ within the range $\Delta a_\mu \pm 2\sigma$. Right: allowed values of ϵ as a function of m_X in the same case. The light gray bands indicate values of ϵ and m_X for which the discrepancy between the theoretical and experimental values of a_μ is less than 2σ . The dark gray regions contain points where the theoretical value of a_μ is at least 2σ larger than the experimental value. The unshaded regions show points where the experimental value of a_μ remains at least 2σ larger than the theoretical value.

Acknowledgments

The author would like to thank J. L. Rosner, Q.-H. Cao, R. J. Hill, D. Krop, A. M. Thalapillil, and P. Draper for discussions and helpful suggestions. This work was supported in part by the United States Department of Energy under Grant No. DE-FG02-90ER40560.

APPENDIX A: Y PAIR PRODUCTION IN e^+e^- COLLISIONS

1. Fermionic Y Production Cross Section

For a fermionic Y , we consider the case where its representation under $SU(2)_L \times U(1)_Y$ is the same as that of the muon. That is, Y_L is a doublet under $SU(2)_L$ with hypercharge -1 while Y_R is an $SU(2)_L$ singlet with hypercharge -2 . Its couplings to the photon and Z boson are then the same as the muon's. The Feynman rule for the electron's (which is the same as the muon's) coupling to the Z boson is shown in Fig. 6. The cross section, ignoring the width of the Z , for $e^+e^- \rightarrow Y\bar{Y}$ is easily found to be

$$\sigma(e^+e^- \rightarrow Y\bar{Y}) = \frac{2\pi\alpha^2}{s}\beta \left\{ \left[1 + \frac{2G^2 a^2}{e^2} \left(\frac{s}{s - m_Z^2} \right) \right] \left(1 - \frac{1}{3}\beta^2 \right) \right. \quad (\text{A1})$$

$$\left. + \frac{G^4 (a^2 + b^2)}{e^4} \left(\frac{s}{s - m_Z^2} \right)^2 \left(a^2 - \frac{1}{2} \left(a^2 - b^2 - \frac{1}{3} \right) \beta^2 \right) \right\} \quad (\text{A2})$$

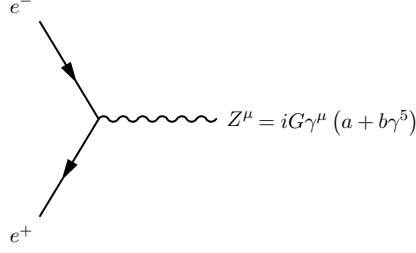


FIG. 6: Feynman rules for the $e^+ - e^- - Z$ vertex (and the $\mu^+ - \mu^- - Z$ vertex). $G = e/(\sin \theta_W \cos \theta_W)$, $a = 1/4 - \sin^2 \theta_W$, and $b = 1/4$ with the weak mixing angle $\sin^2 \theta_W = 0.231$.

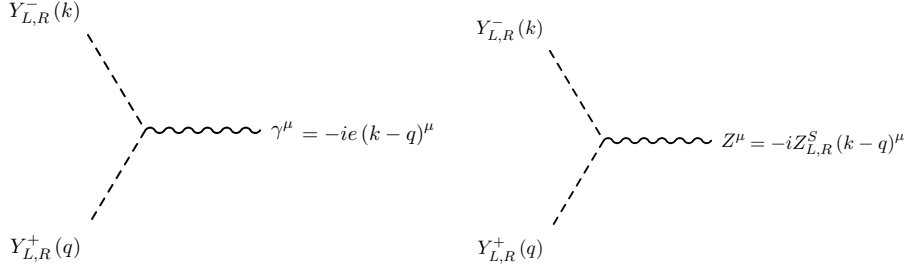


FIG. 7: Feynman rules for a scalar Y . All momenta are running into the graphs. We use $Z_L^S = e(1 - 2\sin^2 \theta_W)/(2\sin \theta_W \cos \theta_W)$ and $Z_R^S = -e \tan \theta_W$.

where G , a , and b , as seen in Fig. 6, are expressed in terms of the electron's charge and the weak mixing angle θ_W as

$$G = \frac{e}{\sin \theta_W \cos \theta_W} \quad , \quad (\text{A3})$$

$$a = \frac{1}{4} - \sin^2 \theta_W \quad , \quad (\text{A4})$$

$$b = \frac{1}{4} \quad . \quad (\text{A5})$$

2. Scalar Y Production Cross Section

For a scalar Y_L we assume that it couples to the Z boson in a gauge invariant way with a strength equal to that of the left-handed muon. We assume analogously for a scalar Y_R . The Feynman rules for these $Y_L - Y_R - \gamma$ and $Y_L - Y_R - Z$ couplings are shown in Fig. 7. We then obtain

$$\sigma(e^+e^- \rightarrow Y_{L,R}^+ Y_{L,R}^-) = \frac{\pi\alpha^2}{s} \left(\frac{\beta^3}{3}\right) \left\{ 1 + \frac{2Ga}{e^2} Z_{L,R}^S \left(\frac{s}{s-m_Z^2}\right) + \frac{G^2(a^2+b^2)}{e^4} (Z_{L,R}^S)^2 \left(\frac{s}{s-m_Z^2}\right)^2 \right\} \quad (\text{A6})$$

where we have again ignored the width of the Z . G , a , and b are as in Eqs. A3-A5 and

$$Z_L^S = \frac{e(1 - 2\sin^2 \theta_W)}{2\sin \theta_W \cos \theta_W} \quad , \quad (\text{A7})$$

$$Z_R^S = -e \tan \theta_W \quad . \quad (\text{A8})$$

3. Vector Y Production Cross Section

To properly determine the cross section for vector Y pair production we need to introduce new states to insure unitarity is not violated. As mentioned in Sec. II, we assume that there is an electrically neutral fermion that couples

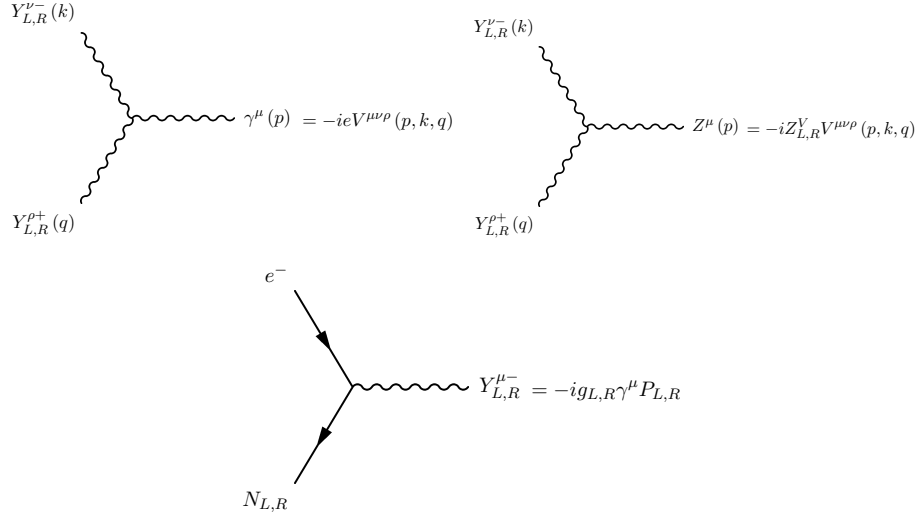


FIG. 8: Feynman rules for a vector Y . $V^{\mu\nu\rho}(p, k, q) = [(p-k)^\rho g^{\mu\nu} + (k-q)^\mu g^{\nu\rho} + (q-p)^\nu g^{\mu\rho}]$ and all momenta are running into the graphs. The photon interaction is fixed by demanding electromagnetic gauge invariance. The values of g_L and $Z_{L,R}^V$ are determined by requiring that they keep Y pair production unitary. They are given in Eq. A23.

to $Y_{L,R}^\nu$ and $e_{L,R}$ which we call $N_{L,R}$. We write the Feynman rules for the interactions of $Y_{L,R}^\nu$ with e^\pm , Z , and $N_{L,R}$ in Fig. 8. The coupling strengths g_L and $Z_{L,R}^V$ will be chosen so that the cross section for $e^+e^- \rightarrow Y_L^{\nu+}Y_L^{\nu-}$ remains finite as $\sqrt{s} \rightarrow \infty$.

We write the cross section for the production of pair of vector Y_L s as

$$\frac{d\sigma}{d\cos\theta}(e^+e^- \rightarrow Y_L^{\nu+}Y_L^{\nu-}) = \frac{\pi\alpha^2\beta}{16s} \sum |\mathcal{M}_{ij}|^2 \quad (\text{A9})$$

where θ is the center-of-mass scattering angle. The squared matrix elements are

$$|\mathcal{M}_{NN}|^2 = \frac{4g_L^4}{e^4} \left(\frac{t}{t-m_{N_L}^2} \right)^2 F_t(t, s) \quad , \quad (\text{A10})$$

$$|\mathcal{M}_{\gamma\gamma}|^2 = F_s(t, s) \quad , \quad (\text{A11})$$

$$|\mathcal{M}_{ZZ}|^2 = \frac{G^2(a^2+b^2)|Z_L^V|^2}{e^4} \left(\frac{s}{s-m_Z^2} \right)^2 F_s(t, s) \quad , \quad (\text{A12})$$

$$|\mathcal{M}_{Z\gamma}|^2 = \frac{2Ga \operatorname{Re}(Z_L^V)}{e^2} \left(\frac{s}{s-m_Z^2} \right) F_s(t, s) \quad , \quad (\text{A13})$$

$$|\mathcal{M}_{NZ}|^2 = -\frac{2G(a+b)\operatorname{Re}(Z_L^V)g_L^2}{e^4} \left(\frac{s}{s-m_Z^2} \right) \left(\frac{t}{t-m_{N_L}^2} \right) F_{st}(t, s) \quad , \quad (\text{A14})$$

$$|\mathcal{M}_{N\gamma}|^2 = -\frac{2g_L^2}{e^2} \left(\frac{t}{t-m_{N_L}^2} \right) F_{st}(t, s) \quad , \quad (\text{A15})$$

where s and t are the usual Mandelstam variables and we have defined the functions

$$F_t(t, s) = 2 \left(\frac{s}{m_{Y_L}^2} \right) + \frac{1}{2}\beta^2 \sin^2[\theta(t)] \left[\left(\frac{s}{t} \right)^2 + \frac{1}{4} \left(\frac{s}{m_{Y_L}^2} \right)^2 \right] \quad , \quad (\text{A16})$$

$$F_s(t, s) = \beta^2 \left\{ 16 \left(\frac{s}{m_{Y_L}^2} \right) + \sin^2[\theta(t)] \left[\left(\frac{s}{m_{Y_L}^2} \right)^2 - 4 \left(\frac{s}{m_{Y_L}^2} \right) + 12 \right] \right\} \quad , \quad (\text{A17})$$

$$F_{st}(t, s) = 16 \left(1 + \frac{m_{Y_L}^2}{t} \right) + 8\beta^2 \left(\frac{s}{m_{Y_L}^2} \right) + \frac{1}{2}\beta^2 \sin^2[\theta(t)] \left[\left(\frac{s}{m_{Y_L}^2} \right)^2 - 2 \left(\frac{s}{m_{Y_L}^2} \right) - 4 \left(\frac{s}{t} \right) \right] \quad . \quad (\text{A18})$$

$$(\text{A19})$$

We relate θ and t through

$$\sin^2 [\theta(t)] = -\frac{4}{\beta^2} \left[\left(\frac{t - m_{Y_L}^2}{s} \right)^2 + \frac{t}{s} \right] . \quad (\text{A20})$$

Unitarity will determine the values of g_L and Z_L^V . Requiring that the coefficients of $(s/m_{Y_L}^2)^2 \sin^2 \theta$ and of $(s/m_{Y_L}^2)$ vanish as $\sqrt{s} \rightarrow \infty$ gives

$$g_L^4 + 2 \left[e^4 + G^2 (a^2 + b^2) |Z_L^V|^2 + 2e^2 G a \operatorname{Re}(Z_L^V) \right] - 2g_L^2 [G(a+b) \operatorname{Re}(Z_L^V) + e^2] = 0 , \quad (\text{A21})$$

while setting the coefficient of $(s/m_{Y_L}^2) \sin^2 \theta$ to zero as $\sqrt{s} \rightarrow \infty$ implies

$$2 \left[e^4 + G^2 (a^2 + b^2) |Z_L^V|^2 + 2e^2 G a \operatorname{Re}(Z_L^V) \right] - g_L^2 [G(a+b) \operatorname{Re}(Z_L^V) + e^2] = 0 . \quad (\text{A22})$$

These two equations are satisfied by

$$g_L^2 = \frac{2e^2 b}{b-a} , \quad Z_L^V = \frac{e^2}{G(b-a)} . \quad (\text{A23})$$

We note that the contribution due to Z boson exchange cannot by itself cancel that from photon exchange unless the Z coupling to electrons is vector-like (which it is not). These conditions allow us to determine $\sigma(e^+e^- \rightarrow Y_L^{\nu+} Y_L^{\nu-})$ as a function of m_{Y_L} and m_{N_L} .

$\sigma(e^+e^- \rightarrow Y_R^{\nu+} Y_R^{\nu-})$ is obtained from $\sigma(e^+e^- \rightarrow Y_L^{\nu+} Y_L^{\nu-})$ by taking $b \rightarrow -b$.

-
- [1] M. Davier, A. Hoecker, B. Malaescu, C. Z. Yuan and Z. Zhang, arXiv:0908.4300 [hep-ph].
[2] J. Prades, E. de Rafael and A. Vainshtein, arXiv:0901.0306 [hep-ph].
[3] G. W. Bennett *et al.* [Muon G-2 Collaboration], Phys. Rev. D **73**, 072003 (2006) [arXiv:hep-ex/0602035].
[4] J. Prades, arXiv:0909.2546 [hep-ph]; F. Jegerlehner and A. Nyffeler, Phys. Rept. **477**, 1 (2009) [arXiv:0902.3360 [hep-ph]]; M. Passera, W. J. Marciano and A. Sirlin, AIP Conf. Proc. **1078**, 378 (2009) [arXiv:0809.4062 [hep-ph]].
[5] F. Domingo and U. Ellwanger, JHEP **0807**, 079 (2008) [arXiv:0806.0733 [hep-ph]]; D. Stockinger, arXiv:0710.2429 [hep-ph].
[6] T. Appelquist and B. A. Dobrescu, Phys. Lett. B **516**, 85 (2001) [arXiv:hep-ph/0106140].
[7] J. A. Conley and J. S. Gainer, arXiv:0811.4168 [hep-ph].
[8] B. Holdom, Phys. Lett. B **166**, 196 (1986); P. Fayet, Nucl. Phys. B **347**, 743 (1990). N. Arkani-Hamed and N. Weiner, JHEP **0812**, 104 (2008) [arXiv:0810.0714 [hep-ph]]; C. Cheung, J. T. Ruderman, L. T. Wang and I. Yavin, Phys. Rev. D **80**, 035008 (2009) [arXiv:0902.3246 [hep-ph]]; A. Katz and R. Sundrum, JHEP **0906**, 003 (2009) [arXiv:0902.3271 [hep-ph]]; D. E. Morrissey, D. Poland and K. M. Zurek, JHEP **0907**, 050 (2009) [arXiv:0904.2567 [hep-ph]].
[9] M. Pospelov, Phys. Rev. D **80**, 095002 (2009) [arXiv:0811.1030 [hep-ph]].
[10] J. L. Feng and J. Kumar, Phys. Rev. Lett. **101**, 231301 (2008) [arXiv:0803.4196 [hep-ph]]; J. L. Feng, H. Tu and H. B. Yu, JCAP **0810**, 043 (2008) [arXiv:0808.2318 [hep-ph]].
[11] J. L. Feng, J. Kumar and L. E. Strigari, Phys. Lett. B **670**, 37 (2008) [arXiv:0806.3746 [hep-ph]].
[12] D. McKeen, Phys. Rev. D **79**, 114001 (2009) [arXiv:0903.4982 [hep-ph]].
[13] A. Heister *et al.* [ALEPH Collaboration], Phys. Lett. B **583**, 247 (2004); J. Abdallah *et al.* [DELPHI Collaboration], Eur. Phys. J. C **31**, 421 (2003) [arXiv:hep-ex/0311019]; P. Achard *et al.* [L3 Collaboration], Phys. Lett. B **580**, 37 (2004) [arXiv:hep-ex/0310007]; G. Abbiendi *et al.* [OPAL Collaboration], Eur. Phys. J. C **32**, 453 (2004) [arXiv:hep-ex/0309014].
[14] O. Adriani *et al.* [PAMELA Collaboration], Nature **458**, 607 (2009) [arXiv:0810.4995 [astro-ph]].
[15] P. Meade, M. Papucci, A. Strumia and T. Volansky, arXiv:0905.0480 [hep-ph].
[16] D. W. Hertzog, Nucl. Phys. Proc. Suppl. **181-182**, 5 (2008); R. M. Carey *et al.*, "The New (g-2) Experiment: A proposal to measure the muon anomalous magnetic moment to ± 0.14 ppm precision"; K. R. Lynch [Muon (g-2) Collaboration], Nucl. Phys. Proc. Suppl. **189**, 201 (2009).